Electrical grid automated visual asset inspection - an example application to PV modules

Pedro Rocha[1]
a21200219@isec.pt
Inacio Fonseca[1]
inacio@isec.pt
Fernando Lopes[1,2]
flopes@isec.pt,flopes@co.it.pt

[1] Polytechnic Institute of Coimbra, Coimbra Institute of Engineering, Coimbra, PT
[2] Instituto de Telecomunicações, Coimbra, PT

Abstract

Periodic inspection of electrical grid assets is fundamental to efficiently manage maintenance activities and guarantee the safe and reliable operation of the grid. For efficient visual inspection, given the huge amounts of collected image data, automated inspection is mandatory. In this paper we investigate a deep learning approach to the automated classification of defects in operating photovoltaic modules through the analysis of outdoor collected thermography images. We test several variants of a simple deep learning architecture on a publicly available dataset of labeled infrared images divided into 12 classes. The classification results yield Precision, Recall and F1-score of 0.87, 0.86 and 0.86, respectively, demonstrating the practical value of the presented automated approach.

1 Introduction

Globally installed solar power exceeded 1000 GW at the end of 2022 with up to 400 GW expected to be installed in 2023 alone [1]. With the rapid expansion of solar photovoltaic (PV) plants, robust and efficient inspection methods are crucial for detecting defects in PV modules and associated systems [2]. Thermographic imaging of PV modules, using thermal infrared (IR) cameras to detect temperature irregularities when compared to healthy ones, has emerged as a valuable inspection approach. To this end, the IEC 62446-3 standard defines outdoor thermographic inspection of PV modules and plants in operation [3]. In the context of the rapidly expanding installation of modern PV systems, manual collection and analysis of images becomes impractical. In practice, huge amounts of images are collected by UAVs equipped with thermal cameras while automated analysis using computer vision with machine learning allows to identify patterns linked to defective modules within thermographic imagery.

2 Literature review

Traditional fault detection methods for PV modules often use classical computer vision techniques. These include binary thresholding for contour extraction and PV module segmentation, as well as obtaining texture features for classification with Support Vector Machines (SVMs). Other approaches involve detecting module edges using morphological operations or the Hough transform. However, these methods have strong limitations. They heavily depend on manual assumptions and heuristics, requiring extensive hyperparameter tuning. They struggle to generalize to new images, making them less adaptable. Moreover, classical algorithms can't handle domain shifts or identify unknown anomalies, limiting their real-world robustness. Despite their historical use, these methods have been largely surpassed by more advanced techniques, particularly using deep learning, which offers accurate and adaptable fault detection solutions. Some representative examples are reviewed here.

Lukas Bommes *et al*. [4] collected a dataset containing millions of RGB and thermographic video frames over seven large PV plants using a UAV equipped with GPS. They developed a tool to map the PV panels using a Mask R-CNN to perform module segmentation and a ResNet-50 deep convolutional classifier to catalog the thermal anomalies in ten classes: Healthy, Open-circuit, Short-circuit, Substring open-circuit, Substring short-circuit, Module PID, Multi hot-cells, Single hot cell, Warm cell(s), Diode overheated and Hot spot. The study demonstrated significant improvements over state-of-the-art methods, achieving a test accuracy exceeding 90% across various plant domains without requiring hyperparameter adjustments.

Jacek Starzyński *et al*. [5] highlighted the impact of radiance deprivation effects, often caused by bird droppings and shadows from vegetation, on a PV module's power output. They used recent DL architectures, including YOLOv4, on a dataset of thermal images collected with UAVs, but revealing modest accuracy. This emphasized the need for data augmentation. The proposed strategy focused on enhancing the Recall score during training to reduce false negatives and perform real-time detections during PV farm overflights, with an adaptive flight path for additional shots from different angles, heights and directions, suggesting a method to address the common scarcity of data examples in defective classes.

In the study led by Yahya Zefri *et al*. [6], PV modules were segmented using images from UAVs. They categorized the modules into six groups: Non-defective module, One hotspot, Patchwork pattern of hotspots, Overheated module row, Overheated module, and Pointed heating. They then compared two models: one they fine-tuned from a pre-trained VGG16 model and another they built from scratch with five convolutional layers. Surprisingly, their own simple model outperformed the more complex VGG16 model, suggesting that the model complexity should match the data complexity to achieve better results.

Ekaterina Engel and Nikita Engel [7] extensively reviewed applications and the performance of machine learning techniques in PV power plants and presented a structured benchmark of recently published articles. Typical applications include modeling and optimizing the design and size of solar plants, as well as forecasting the received irradiance and the generated power through regression. Additionally, reinforcement learning is employed to control the configuration of solar plants and optimize electronic energy conversion, also known as Maximum Power Point Tracking (MPPT). For Maintenance, they reviewed the imagery sensor techniques for failure diagnostics and developed a fault forecasting system based on a Modified Fuzzy Neural Network (MFNN), that was tuned using a two-year historical dataset with signals from a 20 kW PV array.

3 Methodology and implementation

A complete solution for inspecting a PV plant starts with data acquisition, including UAV route planning, followed by video frame cropping to create thermographic images of PV modules. These images are then categorized into different defect classes, ultimately leading to the elaboration of a maintenance report. In this study we focus on the central part of this pipeline system: the computer vision core functions as a sensor that interprets physical quantities and provides valuable calssification information. Our system involves using cropped thermal images of PV modules as input data and generates predictions of defects within one of the 12 classes, according to the used dataset [8] and exemplified in Figure 1 .

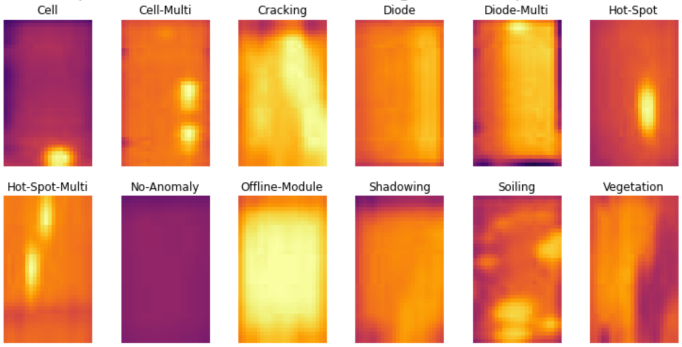

Figure 1: Sample of IR images in 12 classes

3.1 Dataset

From the original dataset, we randomly selected 150 images from each class. Out of these, 100 were reserved for validation and testing. To expand the training dataset we did multiple doubling operations as follows: a 180-degree rotation (2X50); a vertical flip (2x100) and an horizontal flip (2x200). This process yielded a total of 400 images per class for training, across the 12 available classes, amounting to a total of 6000 images (80%, 10%, 10%), when considering all dataset splits.

This option resulted from the recognition that an imbalanced dataset, when used for multi-class classification, can lead to sub-optimal training outcomes. There is a risk that the model might predominantly predict the majority class for most instances, minimizing the overall loss but neglecting the minority classes, overshadowing in the learning process, and affecting the model's ability to discern significant patterns and generate precise predictions across all classes. Figure 2 illustrates the data imbalance before and after the augmentation process.

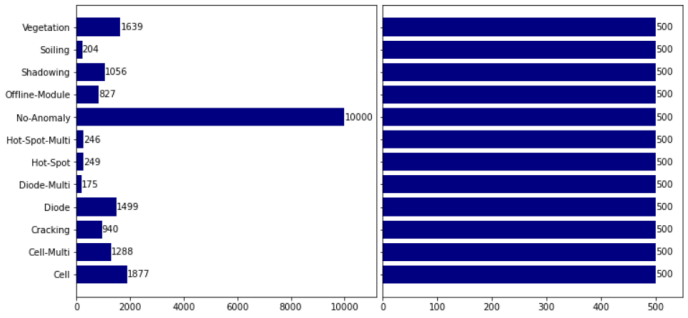

Figure 2: Dataset class counts (original and class augmented)

The augmentation procedure involved only basic operations, such as rotation and mirroring, because other conventional transformations such as cropping, shearing, and adjustments in brightness and contrast have the potential to modify crucial features.

3.2 Architecture and training

Ensuring feature consistency, we maintained the original 40x24 spatial resolution and the 8 bit amplitude resolution of the images in the dataset. We investigate a model architecture based on [6] with structure modifications to better adapt to the used dataset and the features to be identified. Furthermore, our implementation of the architecture in [6] (M1 in Table 1 and Table 2) is used as a reference for performance comparisons. All tested models consist of a block of convolutional layers followed by a block of dense layers. Between these main blocks, there is a flatten layer. The first layer is a normalization layer, and the last dense layer uses *softmax* activation for the 12 classes mentioned above. The convolutional layers use a kernel size of 3x3, with padding set to *same*, and a *stride* of 1 to maintain the output size, or a *stride* of 2 to replace a *maxpooling* layer. ReLU activation is applied to both the Conv2D and dense layers. Table 1 presents a comparison between the different tested architectures.

Table 1: Comparison of model architectures

M	Dimensions of layers	
	Conv2D	Dense
1	40x24x8 - 40x24x8 - 20x12x8 - 20x12x8 - 10x6x8	512 - 512 - 512
2	40x24x32 - 40x24x32 - 20x12x16 - 10x6x16	256 - 512 - 256 - 512
3	40x24x64 - 40x24x32 - 20x12x16	128 - 256 - 128
4	40x24x128 - 40x24x64 - 20x12x32 - 20x12x32	64 - 64 - 64 - 64

The final fine-tuned hyperparameters choice for training lead to a *batch* size of 64, learning rate starting at 0.0025 with a momentum controlled by the *adam* optimizer, regularization applied to the dense layers from an *L2* penalty loss of 0.0001, and the inclusion of dropout layers to mitigate premature overfitting. The evolution of the loss function as a result of the training procedure is presented in Figure 3.

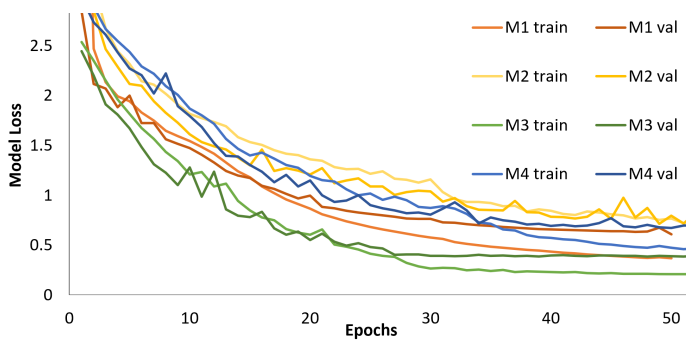

Figure 3: Evolution of the loss function over epochs

4 Results and evaluation

The performance of the tested models, subsequent to loading the corresponding weights before overfitting takes place, is summarized in Table 2 through the calculated Precision, Recall and F1-score. In this application the Recall is considered more relevant since disregarding a false negative has a greater impact than responding to a false positive.

Table 2: Bechmarking of the tested models

M	Precision			Recall			F1-score		
	train	valid	test	train	valid	test	train	valid	test
1	0.70	0.66	0.66	0.69	0.65	0.66	0.68	0.63	0.64
2	0.74	0.68	0.70	0.72	0.67	0.70	0.72	0.66	0.69
3	0.92	0.88	0.87	0.93	0.88	0.86	0.92	0.88	0.86
4	0.84	0.75	0.79	0.83	0.74	0.79	0.83	0.74	0.78

In adition, we obtained the confusion matrix, providing a comprehensive overview of the predictions made by model M3 on the test dataset compared to the actual ground truth labels, as it can be seen in Figure 4. The mispredicted images belong to classes with very similar shapes and features in the limited resolution images.

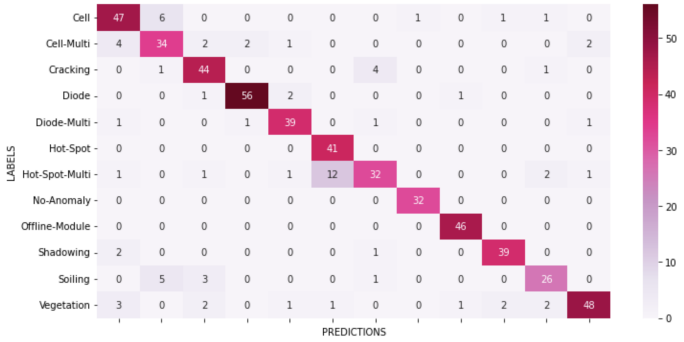

Figure 4: Confusion matrix of the best model (M3)

5 Conclusions and future work

In this work we investigated the use of simple deep learnig models to classify defects in PV modules through the analysis of UAV collected termographic images. The obtained results demonstrate that the proposed model structures are of high practical value in the context of automated electrical grid asset inspection. In future work we intend to improve the model by analysing mispredicted examples and test its adaptability with different datasets. More roboust results can be obtained merging thermography analysis with other sensors such as RGB images and V-I signals.

References

[1] SolarPower Europe. Global market outlook for solar power 2023 - 2027. Technical report, 2022.

[2] Marc Köntges *et al*. Review of failures of photovoltaic modules. Technical report, IEA International Energy Agency, 01 2014.

[3] IEC TS 62446-3:2017. Photovoltaic (PV) systems – Requirements for testing, documentation and maintenance – Part 3: Photovoltaic modules and plants – Outdoor infrared thermography, 2017.

[4] Lukas Bommes, Claudia Buerhop-Lutz, Tobias Pickel, Jens Hauch, Christoph Brabec, and Ian Marius Peters. Georeferencing of photovoltaic modules from aerial infrared videos using structure-from-motion. *Progress in Photovoltaics: Research and Applications*, 30 (9):1122–1135, September 2022.

[5] Jacek Starzyński, Paweł Zawadzki, and Dariusz Harańczyk. Machine Learning in Solar Plants Inspection Automation. *Energies*, 15(16): 5966, January 2022.

[6] Yahya Zefri, Imane Sebari, Hicham Hajji, and Ghassane Aniba. Developing a deep learning-based layer-3 solution for thermal infrared large-scale photovoltaic module inspection from orthorectified big UAV imagery data. *International Journal of Applied Earth Observation and Geoinformation*, 106:102652, February 2022.

[7] Ekaterina Engel and Nikita Engel. A Review on Machine Learning Applications for Solar Plants. *Sensors*, 22(23):9060, January 2022.

[8] Matthew Millendorf, Edward Obropta, and Nikhil Vadhavkar. Infrared solar module dataset for anomaly detection, 2020.